Hindawi
Journal of Spectroscopy
Volume 2022, Article ID 1769710, 6 pages
https://doi.org/10.1155/2022/1769710

Research Article

Spectroscopic Characteristics and Color Origin of Red Tourmaline from Brazil

Ming Li

Jewelry Institute, Guangzhou Panyu Polytechnic, Guangzhou, China

Correspondence should be addressed to Ming Li; lm2020121002@126.com

Received 3 May 2022; Accepted 25 May 2022; Published 6 June 2022

Academic Editor: Davidson Sajan

In the present paper, I report on the spectroscopic study for tourmaline color origin, performed red samples from Minas Geras State, Brazil, by gemological routine testing, X-ray diffraction, Fourier transform infrared spectroscopy, ultraviolet-visible spectroscopy, and X-ray photoelectron spectroscopy. The main goal was the analysis of the optical absorption spectra and the chemical states of transition metal cations in order to better understand the effect of transition metal cations on color of tourmaline. The results showed that the red color was confirmed by the symmetric broad absorption at 527 nm and the narrow absorption at 400 and 450 nm, and the above three absorption bands were caused by the d-d electron transition of Mn^{3+}, which occupied the Y site in the crystal structure and coordinated with F to form bonds. In addition, in principle, the chemical states of the chromogenic ions in tourmaline and their influence on coloration were confirmed, which would be beneficial to assessing the color change and identifying the origin of tourmaline.

1. Introduction

Tourmaline is one of the most popular gem materials. It has the appropriate combination of beauty, durability, and rarity to make fine gemstones. Its moderate refractive index gives significant return of light, its relatively high hardness makes it less likely to be scratched, and its lack of cleavage makes it unlikely to fracture during wear. Especially, its chemical complexity produces a wide range of appealing colors. Perhaps more than any other gemstone, tourmaline is renowned for its spectrum of colors, even within individual crystals. Its rich colors range from colorless, through red, pink, yellow, orange, green, blue, and violet, to brown and black. In the extensive range of colorful gem tourmaline, red tourmaline is a particularly attractive one. Tourmaline is a type of borate-silicate mineral with an extremely complex chemical component and crystal structure. Its general crystal chemical formula is: $XY_3Z_6[Si_6O_{18}][BO_3]_3V_3W$, in which X = Na, Ca, Y = Li, Mg, Fe^{2+}, Mn^{2+}, Al, Cr^{3+}, V^{3+}, Fe^{3+}, Z = Mg, Al, Fe^{3+}, V^{3+}, Cr^{3+}, V = OH, O, and W = OH, F, O; that is, there are extensive isomorphic substitution of ions at X, Y, Z, V, and W sites [1]. The wide variety and intensity of colors are related primarily to color-producing ions in the structure and to exposure to natural radiation [2]. Colorless tourmaline has no or minor transition metal ions [3]. Pink may be caused by the d-d electronic transition of Mn^{2+} in octahedron in crystal structure [4]. Green may be caused by the combined action of Fe^{2+} and Fe^{3+} [5]. Blue is caused by Cu^{2+} and Mn^{3+} [2, 6, 7]. Scholars are also very interested in color causes of red tourmaline and have carried out a lot of research. However, the detailed origin of the color is still nonconclusive. Most of literature reported that the red color in tourmaline has been ascribed to the presence of both Mn^{2+} and Mn^{3+} or a Mn^{2+}-Mn^{3+} charge transfer process [8, 9]. In addition, if the octahedral Y site consists mostly of Mn^{2+} ions, the red color of tourmaline can be weakened [10]. However, some studies observed that some red tourmaline did not contain any Mn [11]. As more studies show, apart from ion species, the occupancy and coordination environment of the same ion in the crystal lattice can also affect the color of tourmaline [12–14]. However, as for the color origin of red tourmaline, there are few in-depth studies on ion occupation and coordination environment except the determination of ion species in the current research work,

which are very important to its color. This paper will take Brazil red tourmaline as the object, study its spectral characteristics using X-ray photoelectron spectroscopy and other spectral methods, reveal its color causes from the perspective of the chemical state of color-induced cations, especially coordination ion and site occupancy, and provide direction reference for its color enhancement.

2. Materials and Methods

The materials for the experiments were a faceted stone (Figure 1(a)), tourmaline powder (Figure 1(b)), crystal sheet (Figure 1(c)), and crystal blocks with freshly cut cross-sections (Figure 1(d)). All samples were prepared from natural red single-crystal raw tourmalines from Minas Geras State, Brazil.

Faceted gemstone is used for refractive index and relative density testing. The powder was used for powder X-ray diffraction (XRD, Bruker D8 ADVANCE) over a scan range from 5° to 65° 2θ with a step size of 0.05°. Fourier transform infrared (FTIR, Bruker Vertex 80) spectroscopy was performed in transmission mode between 4000 and 400 cm^{-1}, with a resolution of 4 cm^{-1} and 32 scans. The powder sample was made into a KBr pellet for collecting the FTIR absorption spectra. The faceted stone was used for ultraviolet-visible spectroscopy (UV-Vis JASCO MSV5200) in transmission mode. The test range was 320–800 nm, with a resolution of 1 nm and a scanning speed of 2000 nm/min. Fresh cross-sections of the crystal were analyzed by X-ray photoelectron spectroscopy (XPS). In order to avoid contamination, the crystal sample was enwrapped with tinfoil and was then broken by a pair of pincers, and the fresh surface was subsequently used for XPS measurement. Test conditions were as follows: Al Kα (E = 1486.6 eV) X-ray radiation source, instrument vacuum better than 5×10^{-7} Pa, scanning step length of 0.05 eV, and counting time of 500 ms. The charge displacement is fixed, and the C1s electron binding energy value (284.8 eV) was used for equipment calibration. The range of energy spectrum was 0–1360 eV. Because the subject of analysis was primarily trace elements, we carefully scanned the photoelectron spectra of these trace elements and repeated 32 times to improve the resolution.

3. Results and Discussion

3.1. Gemological Characteristics. Tourmaline samples are bright red in color and evenly distributed, just as shown in Figure 1. The relative density of the crystal is 2.94. Refractometer tests showed that crystal Ne was 1.624 and No was 1.644.

3.2. X-Ray Diffraction Analysis. Figure 2 presents an XRD pattern of the red tourmaline from Minas Geras State, Brazil.

The strongest observed XRD d-spacings of the powder sample were 6.3190 (101), 4.9395 (021), 4.1932 (211), 3.9668 (220), 3.4436 (012), 2.9312 (122), 2.5610 (051), 2.3313 (511), 2.0255 (223), 1.9057 (342), and 1.4418 (713) Å. The pattern indicated that it is elbaite (a lithium-containing tourmaline) by a comparison with the XRD standard card (PDF49-1833). The XRD peaks were sharp and symmetrical, indicating that the crystallinity of the sample was good [15, 16].

3.3. FTIR Spectroscopy Analysis. FTIR spectrum of the red tourmaline was shown in Figure 3.

The spectrum is consistent with the standard infrared spectrum of elbaite [17], except for the slightly different absorption peaks at 450 and 844 cm^{-1}.

The sample showed an FTIR absorption peak of 450 cm^{-1}. However, this absorption peak is rare or weak within 400–500 cm^{-1} in the common IR spectrum of tourmalines. This peak was assigned to the vibration of the [MO_6] bond between the metal cations and oxygen. Common metal cations include Fe, Mg, and Al, in which the vibration absorption of Mg-O is 470 cm^{-1}, and that of Fe-O is 400 cm^{-1} [18]; there is an obvious gap. Considering the characteristics of Fe, Mg, and Al and their occupancy in the crystal structure, the absorption peak at 450 cm^{-1} may be due to the vibration of the coordination polyhedron Al–O in [AlO_6] [19].

In the range of 500–1110 cm^{-1}, absorption peaks appear at 506, 626, 719, 750, 786, 844, 980, 1025, and 1110 cm^{-1}. A large number of symmetrical absorption peaks can be found in this range, which reflects the vibration of the [Si_6O_{18}] group in the tourmaline crystal structure. The absorption peak at 506 cm^{-1} is caused by the bending vibration (δSi-O) of Si-O; the absorption peaks at 626, 719, 750, and 786 cm^{-1} are due to the symmetrical stretching vibration (ν_sSi–O–Si) of Si–O–Si in the [Si_6O_{18}] group [20]. There is no widely accepted conclusion regarding the 844 cm^{-1} absorption peak, but it is generally still attributed to the symmetric stretching vibration (ν_sSi–O–Si) of Si–O–Si. In addition, the absorption peak at 980 cm^{-1} was assigned to the symmetric stretching vibration (ν_sO–Si–O) of O–Si–O, and the absorption peak at 1025 cm^{-1} was due to the asymmetric stretching vibration (ν_{as}O–Si–O) of O–Si–O. The absorption peak at 1110 cm^{-1} was attributed to the asymmetric stretching vibration (ν_{as}Si–O–Si) of Si–O–Si.

The absorption peaks at 1303 cm^{-1} and 1352 cm^{-1} were assigned to the stretching vibration (νBO_3) of (BO_3) and the bending vibration (δOH) of OH, respectively [21]. The vibrational absorption band of 3000–3800 cm^{-1} is generally associated with the presence of constitution water and adsorbed water. The sample showed double peaks at 3468 cm^{-1} and 3586 cm^{-1}, which were assigned to the vibration (νO3H) of O3H. In addition, a weaker absorption band at 3648 cm^{-1} was attributed to the vibration (νO1H) of O1H [22].

Moreover, the absorption peaks at 3468 cm^{-1}, 3586 cm^{-1}, and 3648 cm^{-1} were assigned to vibrations of H–OH by the presence of the hydrogen bond, which was also confirmed by previous research [23–26].

3.4. UV-Vis Spectroscopy. The red color is a distinctive feature of red tourmaline from Minas Geras State, Brazil. The color structure and absorption bands for the red color were observed in the UV-Vis absorption spectrum of the

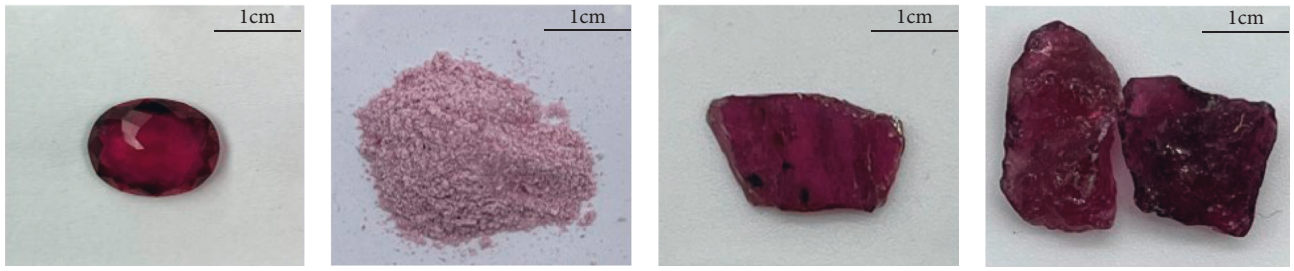

Figure 1: Samples of tourmaline crystal. (a) Faceted stone. (b) Powder. (c) Sheet. (d) Crystal blocks.

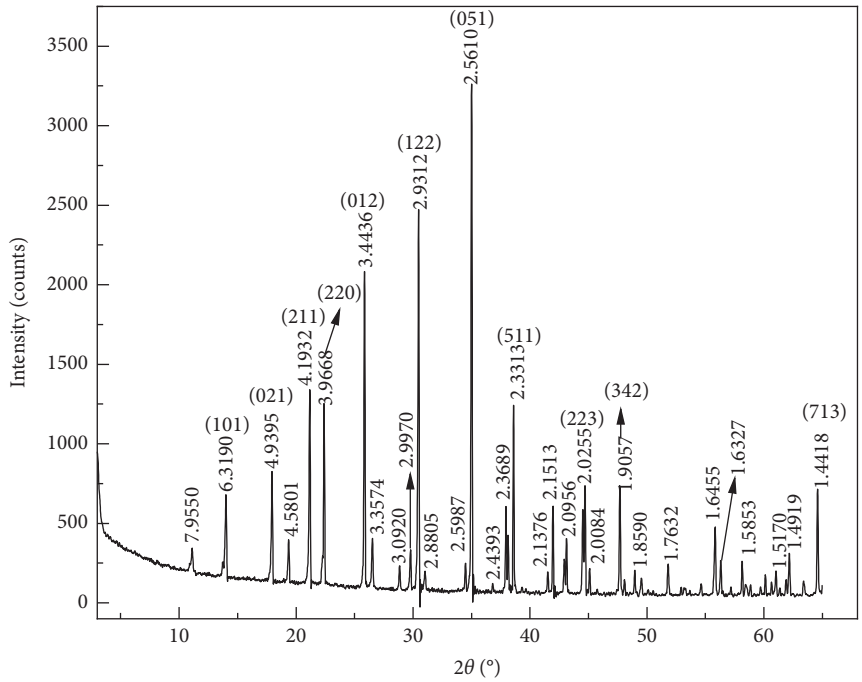

Figure 2: XRD pattern of the tourmaline sample.

sample. Crystals form three typical absorption peaks in the visible region (320–800 nm), namely, the symmetrical wide absorption peak formed at 527 nm in the yellow-green region and the narrower absorption peaks at 400 and 450 nm in the blue-violet region.

Green and blue wavelengths are typically absorbed, and red wavelengths are transmitted, resulting in a red color. However, researchers have disagreements regarding the cause of the absorption peaks at 527, 450, and 400 nm. For example, Wilkins et al. [5] attributed the peak near 520 nm to the combined action of Mn^{2+} and Fe^{3+} by chemical analysis, while more and more studies have shown that the absorption peaks of 527, 450, and 400 nm originate from the d-d electron transitions of Mn^{3+} ions [27–29]. Nevertheless, considering the extensive isomorphic substitution in tourmaline crystals and the vital contribution of variable-valence elements to tourmaline coloration, more chemical data on tourmaline are needed before these peaks can be assigned, especially fine characterization of the chemical states of transition metal cations using XPS. Figure 4 shows the UV-Vis spectrum of the tourmaline sample.

3.5. X-Ray Photoelectron Spectroscopy Analysis. The sample with a fresh cross section was characterized by XPS under a broad-spectrum scan for the element determination in Figure 5. A narrow-spectrum fine scan of the sample was then performed to determine the chemical states of the transition metal elements in Figure 6.

The analysis results showed that the red tourmaline contains mainly Na, Al, Si, O, F, B, and other elements. Through further slow scanning, a small amount of Li and Mn was found, as shown in Figure 6.

The color of tourmaline is often affected by trace transition metal cations [30]. Factors, such as the chemical states of these metal cations and their coordination environment with anions, will change the color of tourmaline [14]. Figure 6 shows the characteristic energy spectrum of

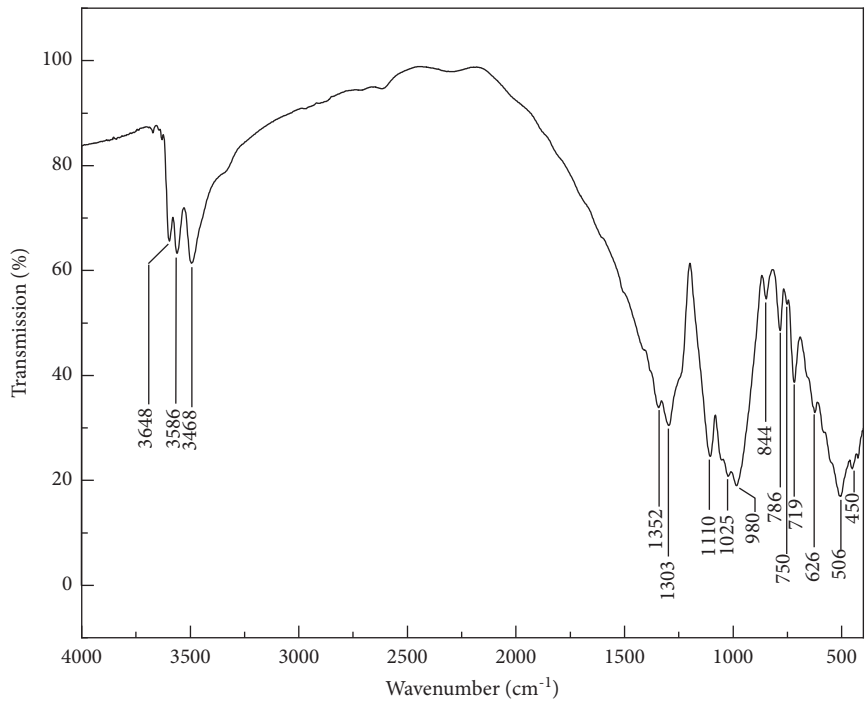

Figure 3: FTIR spectrum of the tourmaline sample.

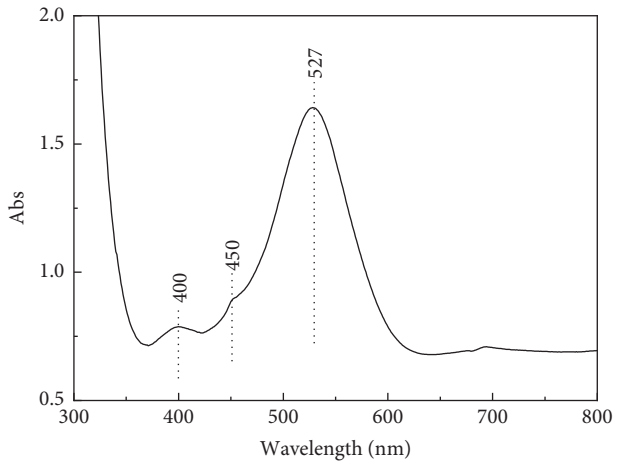

Figure 4: UV-Vis spectrum of the tourmaline sample.

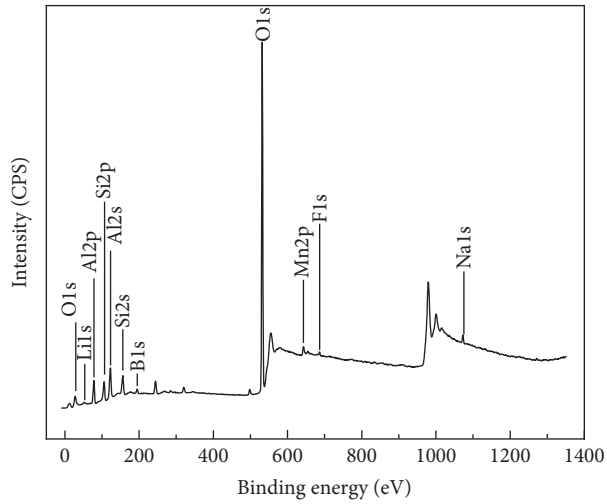

Figure 5: X-ray photoelectron spectrum of the tourmaline sample.

transition metal cations. Figure 6(a) presents the XPS spectrum of Li1s. It shows that the sample contains Li element. This is consistent with the previous XRD and FTIR analysis results. Figure 6(b) presents the XPS spectrum of Mn2p. Mn2p has a highly symmetric peak at 642.3 eV. The electronic binding energy of $Mn2p_{3/2}$ in the sample was comparable to that (642.6 eV) of $Mn2p_{3/2}$ in MnF_3 [31], indicating that Mn in the sample exists in the form of divalent Mn^{3+}, and mainly coordinates with F to form a bond.

In the tourmaline crystal structure, F can only occupy the W site, and the ions at the W lattice site can only coordinate and bond with ions at the Y site instead of the Z site [32]. Therefore, Mn^{3+}, which coordinates and bonds with ions at the F side, occupies the Y site, not the Z site. The color of the tourmaline crystal is related mainly to the absorption caused by the d-electron transition of ions at the Y and Z sites and the charge transfer between the ions sharing edges at the Y and Z sites [30]. Some studies believe that the color is more associated with the nature of ions at the Y site [9]. According to the spectral characteristics of red tourmaline from Brazil, the ion species, and their occupancy in the crystal structure, the color of the red tourmaline was attributed to d-d electron transitionofMn^{3+} occupying the Y site and coordinating with F.

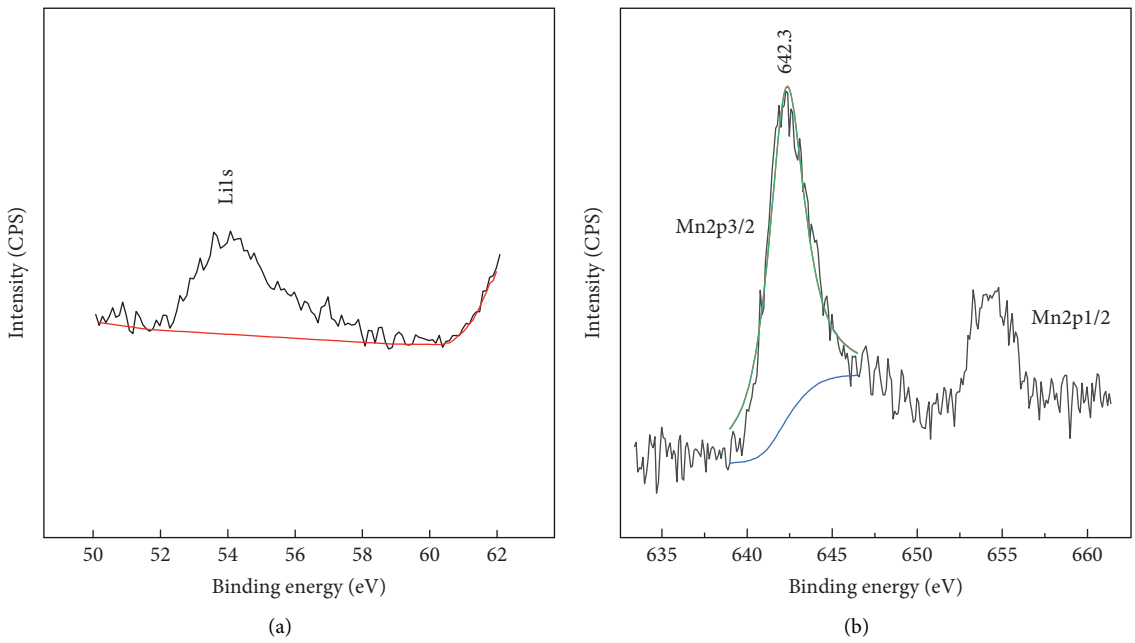

Figure 6: XPS spectra of Li1s and Mn2p. (a) Li1s. (b) Mn2p.

4. Conclusion

The red tourmaline from Minas Geras State, Brazil, is elbaite, exhibiting purple crystal structure from XRD results. The structure of metallic oxide was confirmed by IR spectrum including Mg-O, Fe-O, and the coordination polyhedron Al–O in $[AlO_6]$. The $[Si_6O_{18}]$ group as well as the $[BO_3]$ group was verified by the IR spectrum. The crystal had obvious symmetrical broad absorption at 527 nm in the yellow-green region and vice narrow absorption at 400 and 450 nm in the blue-violet region resulting in present red color. Moreover, the crystal had strong transmission after 630 nm, which brought special optical property for the gem. The XPS results verified d-d electron transition of Mn^{3+} and specified the exact position of Mn^{3+} ion, which occupied the Y site and mainly coordinate with F ions to form bonds.

Data Availability

The data set is presented directly in the present study.

Conflicts of Interest

The author declares that there are no conflicts of interest with any institution or funding body.

Acknowledgments

This work was supported by the Natural Science Foundation of Guangzhou Panyu Polytechnic (Grant no. 2021KJ09).

References

[1] F. C. Hawthorne and D. J. Henrys, "Classification of the minerals of the tourmaline group," *European Journal of Mineralogy*, vol. 11, no. 2, pp. 201–216, 1999.

[2] R. I. Mashkovtsev, S. Z. Smirnov, and J. E. Shigley, "The features of the Cu2+-entry into the structure of tourmaline," *Journal of Structural Chemistry*, vol. 47, no. 2, pp. 252–257, 2006.

[3] F. Pezzotta and B. M. Laurs, "Tourmaline: the kaleidoscopic gemstone," *Elements*, vol. 7, pp. 333–338, 2011.

[4] B. J. Reddy, R. L. Frost, W. N. Martens, D. L. Wain, and J. T. Kloprogge, "Spectroscopic characterization of Mn-rich tourmalines," *Vibrational Spectroscopy*, vol. 44, no. 1, pp. 42–49, 2007.

[5] R. W. T. Wilkins, E. F. Farrell, and C. S. Naiman, "The crystal field spectra and dichroism of tourmaline," *Journal of Physics and Chemistry of Solids*, vol. 30, no. 1, pp. 43–56, 1969.

[6] O. S. Vereshchagin, I. V. Rozhdestvenskaya, O. V. Frank-Kamenetskaya, A. A. Zolotarev, and R. I. Mashkovtsev, "Crystal chemistry of Cu-bearing tourmalines," *American Mineralogist*, vol. 98, no. 8-9, pp. 1610–1616, 2013.

[7] A. Ertl, G. Giester, U. Schüssler et al., "Cu- and Mn-bearing tourmalines from Brazil and Mozambique: crystal structures, chemistry and correlations," *Mineralogy and Petrology*, vol. 107, no. 2, pp. 265–279, 2012.

[8] B. Phichaikamjornwut, S. Pongkrapan, S. Intarasiri, and D. Bootkul, "Conclusive comparison of gamma irradiation and heat treatment for color enhancement of rubellite from Mozambique," *Vibrational Spectroscopy*, vol. 103, Article ID 102926, 2019.

[9] P. G. Manning, "An optical absorption study of the origin of colour and pleochroism in pink and brown tourmalines," *The Canadian Mineralogist*, vol. 9, no. 5, pp. 678–690, 1969.

[10] M. Li, H. Hong, K. Yin, C. Wang, F. Cheng, and Q. J. Fang, "The chemical states of color-induced cations in tourmaline characterized by X-ray photoelectron spectroscopy," *Journal of Spectroscopy*, vol. 2018, Article ID 3964071, 8 pages, 2018.

[11] M. N. Chaudhry and R. A. Howie, "Lithium tourmalines from the meldon aplite, Devonshire, England," *Mineralogical Magazine*, vol. 40, no. 315, pp. 747–751, 1976.

[12] A. Ertl, D. J. Henry, and E. Tillmanns, "Tetrahedral substitutions in tourmaline: a review," *European Journal of Mineralogy*, vol. 30, no. 3, pp. 465–470, 2018.

[13] F. C. Hawthorne, "Short-range atomic arrangements in minerals. I: the minerals of the amphibole, tourmaline and pyroxene supergroups," *European Journal of Mineralogy*, vol. 28, no. 3, pp. 513–536, 2016.

[14] H. L. Hong, J. Li, D. W. Du, Z. Q. Zhong, K. Yin, and C. W. Wang, "Chemical states of color-induced cations in colorful tourmaline," *Journal of Gems & Gemmology*, vol. 13, no. 2, pp. 6–12, 2011.

[15] V. P. Sirotinkin, L. I. Podzorova, N. A. Mikhailina, and O. I. Pen'kova, "X-ray diffraction study of structural changes in high-strength ceramics based on zirconium oxide with additions of ytterbium and neodymium oxides after hydrothermal treatment," *Crystallography Reports*, vol. 67, no. 2, pp. 278–285, 2022.

[16] C. L. Yao and J. M. Zhu, "Mineralization of hydroxyapatite induced by eggshell as calcium source with hydrothermal synthesis method," *Crystallography Reports*, vol. 65, no. 7, pp. 1242–1247, 2020.

[17] W. S. Peng and G. K. Liu, *Mineral Infrared Spectral Atlas*, Science Press, Beijing, China, 1982.

[18] W. W. Liu, R. H. Wu, and Y. Dong, "Study on infrared spectra and infrared radiation characteristics of tourmaline," *Geological Journal of China Universities*, vol. 14, no. 3, pp. 426–432, 2008.

[19] C. F. Zhao, Z. Y. Yin, and B. Li, "Effect of alpha type alumina microstructure on infrared spectra," *Chinese Journal of Spectroscopy Laboratory*, vol. 24, no. 3, pp. 341–344, 2007.

[20] R. Mashkovtsev and A. Lebedev, "IR-Spectroscopic of synthetic in the region of valent oscillations of hydroxyl OH groups," *Soviet Geology and Geophysics*, vol. 32, pp. 80–84, 1991.

[21] T. Gonzales-Carreno, M. Fernandez, and J. Sanz, "Infrared and electron microprobe analysis of tourmaline," *Physics and Chemistry of Minerals*, vol. 15, pp. 452–460, 1988.

[22] C. Castañeda, E. F. Oliveira, N. Gomes, and A. C. P. Soares, "Infrared study of OH sites in tourmaline from the elbaite-schorl series," *American Mineralogist*, vol. 85, no. 10, pp. 1503–1507, 2000.

[23] N. Rekik, N. Issaoui, H. Ghalla, B. Oujia, and M. J. Wójcik, "Infrared spectral density of H-bonds within the strong anharmonic coupling theory: indirect relaxation effect," *Journal of Molecular Structure*, vol. 844-845, pp. 21–31, 2007.

[24] N. Rekik, H. Ghalla, N. Issaoui, B. Oujia, and M. J. Wójcik, "Infrared spectral density of hydrogen bonds within the strong anharmonic coupling theory: quadratic dependence of the angular frequency and the equilibrium position of the fast mode," *Journal of Molecular Structure: THEOCHEM*, vol. 821, no. 1–3, pp. 58–70, 2007.

[25] N. Rekik, N. Issaoui, B. Oujia, and M. J. Wójcik, "Theoretical IR spectral density of H-bond in liquid phase: combined effects of anharmonicities, Fermi resonances, direct and indirect relaxations," *Journal of Molecular Liquids*, vol. 141, no. 3, pp. 104–109, 2008.

[26] N. Issaoui, H. Ghalla, S. A. Brandan et al., "Experimental FTIR and FT-Raman and theoretical studies on the molecular structures of monomer and dimer of 3-thiopheneacrylic acid," *Journal of Molecular Structure*, vol. 1135, pp. 209–221, 2017.

[27] P. G. Manning, "Effect of second-nearest-neighbour interaction on Mn3+ absorption in pink and black tourmalines," *The Canadian Mineralogist*, vol. 11, pp. 971–977, 1973.

[28] Y. Fuchs, M. Lagache, and J. Linares, "Oxydation expérimentale de Fe-tourmalines et corrélation avec une déprotonation des groupeshydoxyle," *Comptes Rendus Geoscience*, vol. 334, no. 4, pp. 245–249, 2002.

[29] K. Krambrock, M. Pinheiro, S. Medeiros, K. Guedes, S. Schweizer, and J. M. Spaeth, "Investigation of radiation-induced yellow color in tourmaline by magnetic resonance," *Nuclear Instruments and Methods in Physics Research Section B: Beam Interactions with Materials and Atoms*, vol. 191, no. 1–4, pp. 241–245, 2002.

[30] K. Nassau, "The origins of color in minerals," *American Mineralogist*, vol. 63, no. 3-4, pp. 219–229, 1978.

[31] J. C. Carver, G. K. Schweitzer, and T. A. Carlson, "Use of X-ray photoelectron spectroscopy to study bonding in Cr, Mn, Fe, and Co compounds," *The Journal of Chemical Physics*, vol. 57, no. 2, pp. 973–982, 1972.

[32] H. Skogby, F. Bosi, and P. Lazor, "Short-range order in tourmaline: a vibrational spectroscopic approach to elbaite," *Physics and Chemistry of Minerals*, vol. 39, no. 10, pp. 811–816, 2012.